Journal of Applied Polymer Science

In situ incorporation of monodisperse drug nanoparticles into hydrogel scaffolds for hydrophobic drug release

JingJing Zhang,[1] LiSheng Zhao,[2] JianJun Zhang,[1] ZhiBing Zhang,[3] Yuan Le,[1,3] Ning Wen,[2] JieXin Wang[1,3]

[1]State Key Laboratory of Organic-Inorganic Composites, Beijing University of Chemical Technology, Beijing, 100029, People's Republic of China

[2]Department of the Prosthodontics, the General Hospital of Chinese PLA, Beijing, 100853, People's Republic of China

[3]Research Center of the Ministry of Education for High Gravity Engineering and Technology, Beijing University of Chemical Technology, Beijing, 100029, People's Republic of China

Correspondence to: J.-X. Wang (E-mail: wangjx@mail.buct.edu.cn) and N. Wen (E-mail: wenning@foxmail.com)

ABSTRACT: The effective and locally sustained delivery of hydrophobic drug with hydrogels as carriers is still a challenge owing to the inherent incompatibility of hydrophilic hydrogel network and hydrophobic drug. One promising approach is to use porous hydrogels to encapsulate and deliver hydrophobic drug in the form of nanoparticles to the disease sites. However, this approach is currently limited by the inability to load concentrated hydrophobic drug nanoparticles into the hydrogels because of the severe nanoparticle aggregation during the loading process. In this article, we firstly designed and fabricated efficient drug nanoparticles embedded hydrogels for hydrophobic drug delivery by incorporating monodisperse silybin (hydrophobic drug for liver protection) nanoparticles into acrylated hyaluronic acid (HA-AC) based hydrogels through *in situ* cross-linking. The silybin nanoparticles embedded hydrogel scaffolds proved to be a good sustained release system with a long period of 36 h. The drug release from this hybrid hydrogels could be modulated by tuning HA-AC concentration, cross-linking ratio, chain length of cross-linker and drug loading amount. The different kinetic models were applied, and it was observed that the release profile of silybin best followed the Hixson-Crowell model for the release of drug from the hydrogels embedding silybin nanoparticles. It could be envisioned that this process would significantly advance the potential applications of hydrogel scaffolds mediated hydrophobic drug delivery in clinical therapies. © 2015 Wiley Periodicals, Inc. J. Appl. Polym. Sci. **2016**, *133*, 43111.

KEYWORDS: biopolymers & renewable polymers; drug delivery systems; nanoparticles; nanowires and nanocrystals

Received 7 July 2015; accepted 30 October 2015

DOI: 10.1002/app.43111

INTRODUCTION

Hydrogels are three-dimensional networks of cross-linked polymers, which can absorb and retain a great quantity of water and biological fluids without being dissolved. Various hydrogels have found wide applications in a variety of biomedical fields, such as drug delivery system,[1–5] tissue engineering,[5–7] imaging,[8] therapeutics,[9,10] and medical devices[1,11] because of their resemblance of natural living tissue and inherent biocompatibility. Among them, injectable and biodegradable hydrogels have received the most considerable attention.[12–14]

Presently, the unique physical properties of hydrogels have sparked particular interest in their use in drug delivery applications. Their highly porous structure can easily be tuned by controlling the cross-linking density in the gel matrix and the affinity of the hydrogels for the aqueous environment in which they are swollen. Their porosity also permits loading of drugs into the gel matrix and subsequent drug release at a rate dependent on the diffusion coefficient of the small molecule or macromolecule through the gel network. Indeed, the benefits of hydrogels for drug delivery may be largely pharmacokinetic – specifically that a depot formulation is created from which drugs slowly elute, maintaining a high local concentration of drug in the surrounding tissues over an extended period, although they can also be used for systemic delivery.[1]

Classically, hydrogels have been used to deliver hydrophilic drugs which have high solubilities in both the hydrophilic hydrogel matrix and the aqueous solvent swelling the hydrogel. In this case, it is relatively simple to load a high quantity of drug into a swollen hydrogel by simple partitioning from a concentrated aqueous drug solution and subsequently release the hydrophilic drug payload into an aqueous environment.

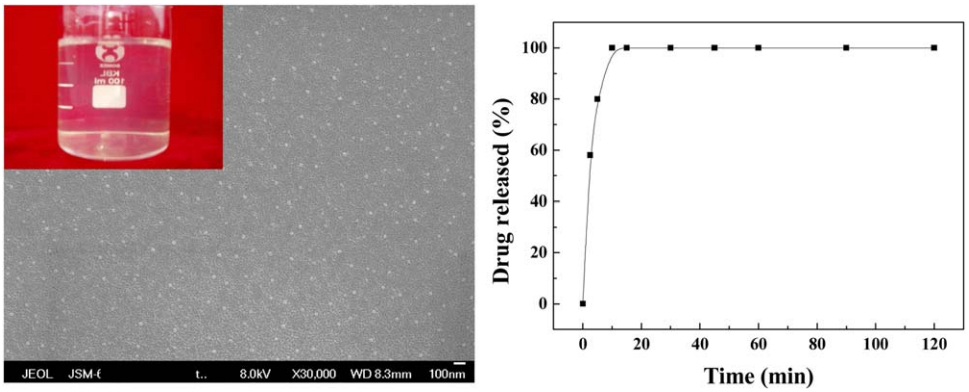

Figure 1. SEM image of the used SLB drug nanoparticles (inset: photo of aqueous nanodispersion) and the dissolution curve of SLB nanoparticles. [Color figure can be viewed in the online issue, which is available at wileyonlinelibrary.com.]

However, this process is relatively inefficient in the case of hydrophobic drugs which are sparingly soluble in both the aqueous and the hydrogel phases. Hydrogel-based hydrophobic drug delivery is in many respects a more difficult problem given the inherent incompatibility of the hydrophilic hydrogel network and the hydrophobic drug. Thus, the problem of hydrophobic drug delivery is two-fold: how to load the hydrophobic drug into the gel matrix and, once present, how to effectively release the drug into the aqueous gel environment.[1] To overcome this problem, hydrophobic drug is commonly encapsulated in a secondary controlled release vehicle such as surfactant-stabilized microemulsion droplet,[15] surfactant micelle,[16,17] and polymeric micelle,[18] which is further entrapped in hydrogel networks to provide prolonged drug release. However, this route may result in a low drug loading amount in the hydrogels owing to the employment of secondary vehicles.

Nanoparticles are well known to improve the dissolution rate and bioavailability of hydrophobic drugs owing to increased surface area available for dissolution as described by the Noyes-Whitney equation.[19] One promising idea is to use hydrogel scaffolds to encapsulate and deliver hydrophobic drug in the form of nanoparticles to the disease sites. However, this is currently limited by the inability to load concentrated hydrophobic drug nanoparticles into the hydrogels because of the severe nanoparticle aggregation during the loading process. Therefore, our approach is to firstly make hydrophobic drug nanoparticles well dispersed in aqueous solution by a rapid precipitation of raw drug, followed by the *in situ* incorporation of nanoparticles into injectable acrylated hyaluronic acid based hydrogel networks with meshes of tens of nanometer by covalent cross-linking. With this strategy, hydrophobic drug nanoparticles can be bound strongly to the polymer chains or meshes in the hydrogel network, effectively realizing a good sustained release of hydrophobic drug. Such a drug delivery system can accomplish the following objectives: (1) achieve highly concentrated and homogeneous loading of hydrophobic drug in hydrogel scaffolds; (2) regulate the dissolution rate of hydrophobic drug by tuning highly porous structure and drug loading amount; (3) realize effective and sustained delivery of hydrophobic drug locally directed in the disease sites by selecting suitable hydrogels.

EXPERIMENTAL

Chemicals

The raw drug of silybin (purity: 98.6%) was purchased from Panjin Huacheng Pharmaceutical. Polyvinylpyrrolidone K30 (PVP) was obtained from Beijing Yili Fine Chemicals. Sodium dodecyl sulphate (SDS) was supplied by Tianjin Bodi Chemical Reagent Company. Tween-80 and acetone were of analytical grade and provided commercially by Beijing Chemical Works. Hyaluronic acid (HA) and adipic dihydrazide (ADH) were purchased from Genscript; 1-ethyl-3-[3-dimethylaminopropyl] carbodiimide hydrochloride (EDC) and N-acryloxysuccinimide (NHS-AC) were bought from Enzyme Research Laboratories and Polysciences, respectively. 1, 4-dithiothreitol ($C_4H_{10}O_2S_2$, $SHCH_2CHOH$-$CHOHCH_2SH$, M (molecular weight) = 154) as short chain cross-linker and double thiolated polyethylene glycol (SH-PEG-SH, $SHCH_2CH_2O(CH_2CH_2O)_nCH_2CH_2SH$, $M = 3500$) as long-chain cross-linker were obtained from Genlantis and BD Biosciences, respectively. Deionized water was purified by Hitech-K Flow Water Purification System (Hitech instruments, Shanghai, China).

Preparation of Monodisperse Hydrophobic Drug Nanoparticles

In this study, silybin as a therapeutic agent for a variety of acute and chronic liver diseases was adopted as model drug. For a typical synthesis procedure of silybin nanoparticles, 1.0 g raw silybin was dissolved in 50 mL acetone (2 wt %). The formed drug solution was rapidly added into 500 mL deionized water containing PVP and SDS (The concentrations of PVP and SDS in water: PVP=1 wt %; SDS=0.006 wt %) as antisolvent ($V_{anti\text{-}solvent}/V_{solvent}=10$). After stirring for 30 s, the precipitated nanosuspension containing silybin nanoparticles was obtained, and then processed by spray drying to generate silybin nanocomposite particles. Upon the exposure of silybin solid dispersion to aqueous media, the stable transparent silybin aqueous nanodispersion containing the water redispersible silybin nanoparticles was thus formed. SEM image of silybin nanoparticles, digital photograph of transparent silybin aqueous nanodispersion and the corresponding dissolution curve were shown in Figure 1. The detailed preparation process could be referred in our previous publication.[20] The silybin aqueous nanodispersion was

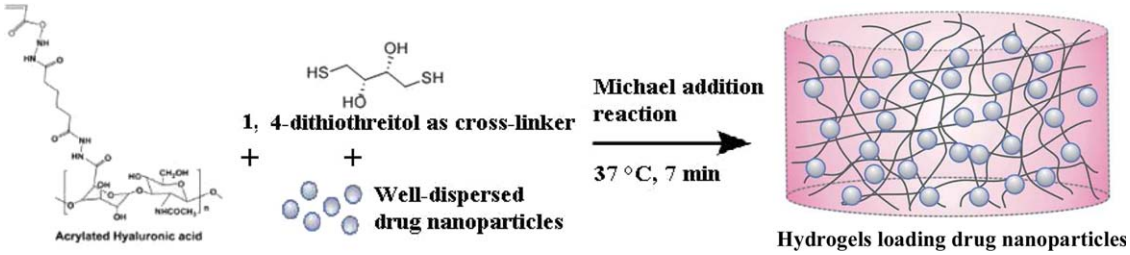

Figure 2. Scheme for *in situ* encapsulation of well-dispersed hydrophobic drug nanoparticles within HA-AC based hydrogels formed by a Michael addition reaction. [Color figure can be viewed in the online issue, which is available at wileyonlinelibrary.com.]

transparent, which had good particle dispersity and stability, an average particle size of about 30 nm, as well as a fast 100% drug dissolution in 10 min.

Hyaluronic Acid Modification

Acrylated hyaluronic acid (HA-AC) was prepared using a reported two-step synthesis.[21] Hyaluronic acid (2.0 g, 60 kDa) was reacted with 25.0 g adipic dihydrazide (ADH) at a pH value of 4.75 in the presence of 4.0 g 1-ethyl-3-[3-dimethylaminopropyl] carbodiimide hydrochloride (EDC) overnight and purified through dialysis (8000 MWCO) in deionized water for 3 days. The purified intermediate (HA-ADH) was freeze-dried and stored at −20°C until used. 37.8% of the carboxyl groups were modified with ADH based on the trinitrobenzene sulfonic acid (TNBSA, Pierce, Rockford, Illinois) assay. HA-ADH (1.9 g) was reacted with N-Acryloxysuccinimide (1.33 g) in HEPES buffer (pH 7.2) overnight and purified through dialysis in deionized water for 3 days before freeze-drying. All the primary amines were acrylated based on the TNBSA assay.

Preparation of HA-AC Hydrogels Embedding Monodisperse Silybin Nanoparticles

After obtaining HA-AC by the above hyaluronic acid modification, HA-AC hydrogels embedding monodisperse silybin nanoparticles were achieved with an *in situ* cross-linking method by adding monodisperse hydrophobic drug nanoparticles during the gelation process of HA-AC based hydrogels. Figure 2 presents a scheme for *in situ* encapsulation of well-dispersed drug nanoparticles within HA-AC based hydrogels formed by a Michael addition reaction with an example of 1, 4-dithiothreitol as cross-linker. Typically, 100 mg of HA-AC was firstly dissolved in 1.2 mL of $NaHCO_3$ buffer solution. Afterwards, 121 mg of silybin nanocomposite powder containing 20 mg of silybin nanoparticles was dispersed in 400 μL of $NaHCO_3$ buffer solution to form the suspension. The above solution and suspension were completely mixed. Simultaneously, 5.78 mg of 1, 4-dithiothreitol as cross-linker was also dissolved in another 400 μL of $NaHCO_3$ buffer solution. A Michael addition reaction took place at 37°C by mixing the suspension containing HA-AC and well-dispersed drug nanoparticles, as well as the solution containing cross-linker, thereby forming bulk phase HA-AC based hydrogels loading silybin nanoparticles after 7 min. Finally, the as-prepared hybrid hydrogels were immersed into liquid nitrogen and freeze-dried for use.

Characterization

SEM images were obtained through a scanning electron microscopy (SEM) (JSM-6701, JEOL, Japan). The spatial distribution of fluorescent drug nanoparticles within the cross-linked hydrogel scaffolds was visualized with a confocal microscope (TCS SP5, Lecia, Germany). Dissolution testing was carried out following the USP Apparatus 2 (paddle) method (D-800LS, Tianjin, China). The paddle speed and bath temperature were set at 100 rpm and (37.0 ± 0.5)°C, respectively. Tween-80 (0.5 wt %) aqueous solution was employed as the dissolution medium. A given amount of HA hydrogels loading drug nanoparticles was added into the vessel containing 500 mL dissolution medium. 5 mL aliquot was withdrawn each time at specific intervals and filtered through a 0.22 μm syringe filter. The concentration of the sample was assayed by a UV spectrophotometer (UV-2501, Shimadzu, Japan) at 287 nm. Each sample was analyzed in triplicate. The standard curve, whose equation was shown as followed, was linear ($r^2 = 0.9999$) in the range from 0 to 80 μg/mL.

$$y = 21.785x - 0.0209$$

where x was absorbency, and y was concentration of silybin, μg/mL.

RESULTS AND DISCUSSION

Figure 3 shows a photograph of freshly prepared blank hydrogels and hydrogels loading well-dispersed silybin (SLB) nanoparticles, SEM images of blank hydrogels and the hydrogels loading SLB nanoparticles after freeze-drying, and confocal microscope image for the spatial distribution of fluorescent drug nanoparticles within hydrogel hybrid scaffolds. Clearly, blank hydrogels were white while the HA-AC hydrogels loading SLB nanoparticles appeared faint yellow owing to the addition of drug nanoparticles. And they had no fluid properties under gravity, thereby forming bulk phase hydrogels after the gelation time of 7 min. After freeze-drying, hydrogels had a fine network structure with lots of microsized pores [Figure 3(B)]. When immersed in water, hydrogels swelled and microsized pores significantly shrank as meshes with tens of nanometer, which was similarly reported.[22] These meshes could effectively accommodate and confine drug nanoparticles with a size of 30 nm. In addition, it could be seen that there were well-dispersed small particles (white dots) in microsized pores of freeze-dried hydrogels, belonging to silybin nanoparticles [Figure 3(C,D)]. To clearer exhibit the spatial distribution of drug nanoparticles in the hydrogels, fluorescein-conjugated silybin nanoparticles were obtained by the addition of 10 mg fluorescein in the preparation process of silybin nanoparticles. The small red dots in a confocal microscope image [Figure 3(E)] emerged as a uniform distribution, proving a good and homogenous loading of drug nanoparticles throughout the HA-AC hydrogels with our route.

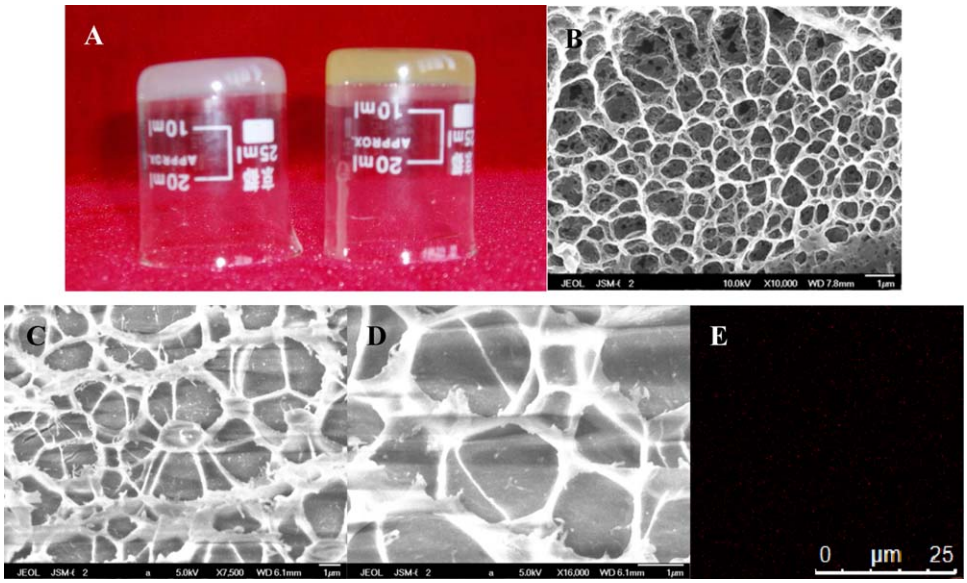

Figure 3. Photograph (A) of freshly prepared blank hydrogel (left) and hydrogel loading SLB drug nanoparticles (right), SEM images of blank hydrogel (B) and the hydrogel loading SLB drug nanoparticles after freeze-drying (C,D), and confocal microscope image (E) for the spatial distribution of fluorescent drug nanoparticles within hydrogel hybrid scaffolds. [Color figure can be viewed in the online issue, which is available at wileyonlinelibrary.com.]

The porous network structure of hydrogel has a very crucial effect on drug release from the hydrogel-nanoparticles (NPs) hybrid scaffolds. We could modulate the highly porous structure of hydrogel-NPs hybrid scaffolds by varying HA-AC concentration, cross-linking ratio and chain length of cross-linker. Figure 4 gives the effect of HA-AC concentration on cumulative SLB release from the hydrogel-NPs hybrid scaffolds at 100% cross-linking ratio. For three HA-AC concentrations, there were first rapid and then slow release processes. With the increase of HA-AC concentration, drug release obviously became slow. At 6 h, the percentages of cumulative drug released for 3%, 5% and 8% were 78%, 64%, and 28% respectively. This is because higher HA-AC concentration is beneficial to the formation of tightly cross-linked hydrogels with a higher cross-linking density as well as the corresponding smaller mesh size and longer degradation time. These will have an important combined effect on SLB release kinetics from hydrogel-NPs hybrid scaffolds, thereby greatly limiting drug delivery.

Figure 5 presents the effect of cross-linking ratio on cumulative SLB release from the hydrogel-NPs hybrid scaffolds. These data indicated a clear-cut dependence on cross-linking ratio. The hydrogel-NPs hybrid scaffolds had a decreased release rate with the increased cross-linking ratio from 25% to 100%. Compared to the cross-linking ratio of 25% or 50%, the complete (100%) cross-linking of hydrogels could form the compacter network structure, thereby effectively delaying drug delivery with a reduced degree of drug release by 10–20%. This also indicated that the loosely formed polymer matrix at lower cross-linking could release drug faster than the tightly formed matrix at

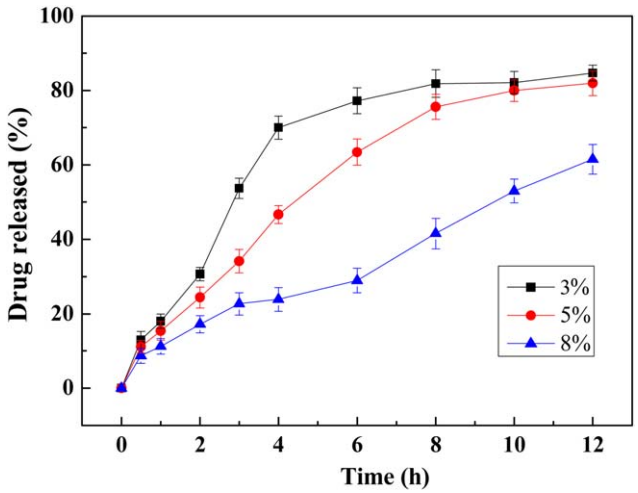

Figure 4. Effect of HA-AC concentration on cumulative SLB release from the hydrogel-NPs hybrid scaffolds. [Color figure can be viewed in the online issue, which is available at wileyonlinelibrary.com.]

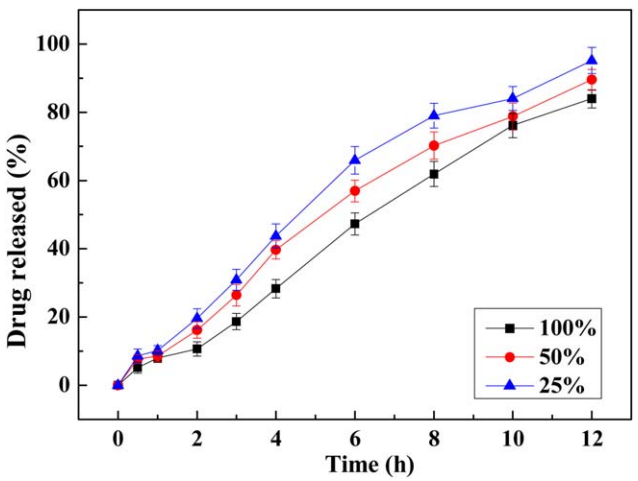

Figure 5. Effect of cross-linking ratio on cumulative SLB release from the hydrogel-NPs hybrid scaffolds. [Color figure can be viewed in the online issue, which is available at wileyonlinelibrary.com.]

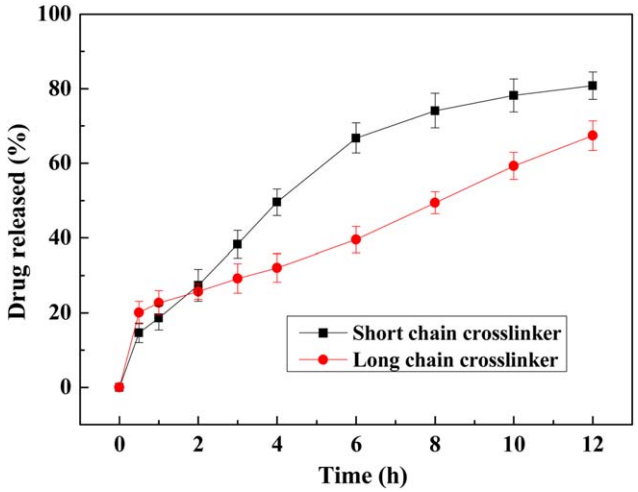

Figure 6. Effect of chain length of cross-linker on cumulative SLB release from the hydrogel-NPs hybrid scaffolds. [Color figure can be viewed in the online issue, which is available at wileyonlinelibrary.com.]

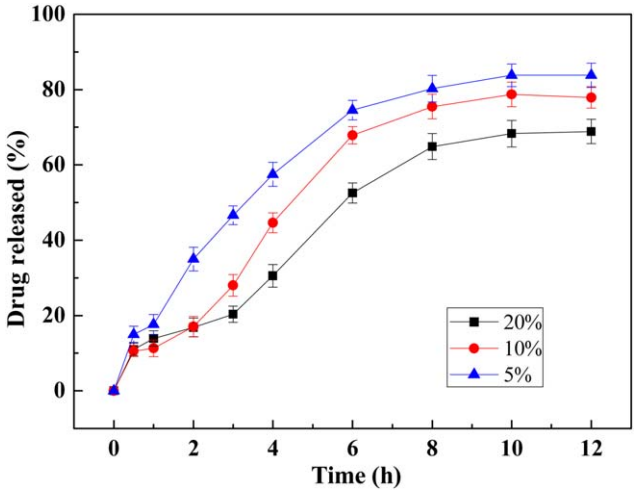

Figure 7. Effect of drug loading amount on cumulative SLB release from the hydrogel-NPs hybrid scaffolds. [Color figure can be viewed in the online issue, which is available at wileyonlinelibrary.com.]

higher cross-linking. However, the effect of cross-linking ratio is much smaller than that of HA-AC concentration.

Figure 6 shows the effect of chain length of cross-linker on cumulative SLB release from the hydrogel-NPs hybrid scaffolds. The hybrid hydrogels prepared with long-chain cross-linker had a first faster and then obviously reduced slower release rate than the counterpart. It is well-known that long-chain cross-linker could form the hydrogels with the relatively larger mesh size and thicker polymer chains. The larger mesh size is beneficial to the dissolution process. However, the hydrogels with thicker polymer chains are harder to degradation, thereby hindering the drug release. Obviously, in this case, the former reason initially plays a major role but afterwards, the latter has a more significant effect.

Besides the porous structure of hydrogels, drug loading amount also has an effect on drug controlled release from the hydrogel-NPs hybrid scaffolds. Figure 7 displays the effect of drug loading amount on cumulative SLB release from the hydrogel-NPs hybrid scaffolds. It was evident that the samples with different drug loading amounts had the similar release rates at the first 30 min owing to the similar loading status of drug nanoparticles in the hydrogel scaffolds. However, after 30 min, drug released percentage decreased with the increased drug loading amount from 5% to 20%. This is because higher drug loading will release more drug molecules, thereby resulting in a higher drug concentration in the dissolution medium. This will have a more and more apparent limitation to the drug release rate with time. So the hybrid hydrogels with a drug loading amount of 20% last a longer release time.

Figure 8 gives a typical cumulative drug release curve from the hydrogel-NPs hybrid scaffolds prepared under an optimum condition. There was no obvious burst release but a gradual slower release process, lasting a long period of 36 h. The hybrid hydrogels exhibited an excellent sustained release property, clearly demonstrating the good feasibility of incorporating well-dispersed hydrophobic drug nanoparitcles into hydrogel network scaffolds for sustained release. It could be concluded that this route not only overcomes the difficulties of incorporating raw drug with tens of micrometer into hydrogels with meshes of tens of nanometer and the severe nanoparticle aggregation during the incorporation process, but also achieves a shift from a rapid complete dissolution (10 min, as shown in Figure 1) of originally separate drug nanoparticles to a good delayed release (36 h) of drug nanoparticles embedded in highly porous hydrogel network. In addition, the formed HA-AC hydrogels were completely degraded after about 100 h, much longer than the drug release period of 36 h. Obviously, the degradation of hydrogel matrix will have a continuous and important effect during the whole drug release period.

To further study the release kinetics of the hydrogel-NPs hybrid scaffolds, some commonly used empirical equations[23,24] shown in Table I were applied to drug release data obtained. Table I exhibits curve fitting results of the release data for various equations. From the analysis of release kinetics using empirical equations, it was found that the fit was better with the Hixson-

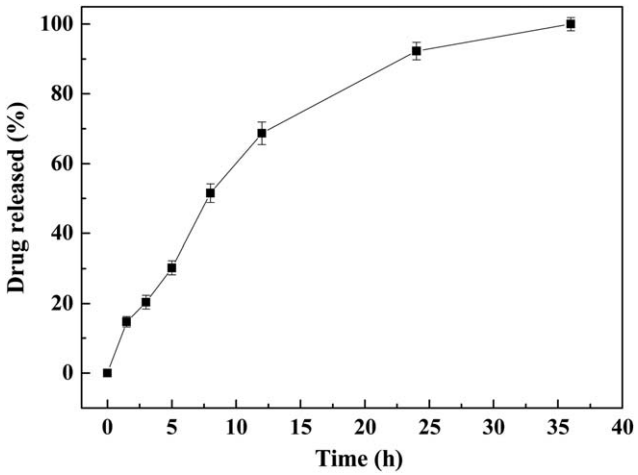

Figure 8. Cumulative drug release curve from the hydrogel-NPs hybrid scaffolds prepared under an optimum condition (1, 4-dithiothreitol as cross-linker, HA-AC concentration of 8%, cross-linking ratio of 100% and drug loading amount of 20%.)

Table I. Curve Fitting Results of the Release Data for Various Equations

Model	Equation	R^2 (Regression coefficient)	S (Residual sum of square)
Zero-order	$Q = kt + b$	0.98346	105.43883
First-order	$\ln(100 - Q) = -kt + b$	0.97589	0.05839
Higuchi	$Q = kt^{1/2} + b$	0.93133	437.8896
Ritger-Peppas	$\ln Q = k\ln t + b$	0.96544	0.15257
Weibull	$\ln(\ln(100/(100 - Q))) = kt + b$	0.95294	0.34221
Hixson-Crowell	$(100 - Q)^{1/3} = -kt + b$	0.98522	0.05286

where Q (%) is the percentage of cumulative drug release at time (t), k is the rate constant of drug release, and b is the constant.

Crowell kinetic model than with the other equations because of the largest value of regression coefficient (R^2) and the smallest value of residual sum of square (S). This suggested that the release kinetics possibly followed the Hixson-Crowell cube-root equation, which is usually suitable for the release process mainly limited by the dissolution rate of drug particles, not the diffusion rate of drug in polymer. Therefore, it can be deduced that the whole drug release process in this system may be controlled by the dissolution of hydrophobic drug nanoparticles strongly bound to the polymer chains or meshes in the HA-AC hydrogel network and the degradation of the hydrophilic HA-AC hydrogel matrix.

CONCLUSIONS

In summary, we successfully developed a novel hydrogel-based delivery system for controlled release of hydrophobic drug of silybin for liver protection by incorporating well-dispersed hydrophobic drug nanoparticles in water into HA-AC based hydrogels through *in situ* cross-linking. The hybrid hydrogel scaffolds loading monodisperse silybin nanoparticles exhibited an excellent sustained release with a period of 36 h. The increase of HA-AC concentration and cross-linking ratio was beneficial to the formation of hydrogels with a higher cross-linking density and the corresponding smaller mesh size, thereby achieving a better delayed release. Longer chain cross-linker and higher drug loading amount could also prolong drug delivery. The drug release kinetics was analyzed using different empirical equations, best following the Hixson-Crowell model. The strategy reported here offers a new direction to engineer hydrophobic drug delivery system based on monodisperse drug nanoparticles embedded hydrogels in clinical therapies.

ACKNOWLEDGMENTS

This work was financially supported by National Natural Science Foundation of China (51303009), National "863" Program of China (2013AA032201), National Key Basic Reasearch Program of China (2015CB932100), Program for New Century Excellent Talents in University of China (NCET-12-0760), and Beijing Higher Education Young Elite Teacher Project (YETP0485).

REFERENCES

1. Hoare, T. R.; Kohane, D. S. *Polymer* **2008**, *4949*, 1993.
2. Das, D.; Das, R.; Mandal, J.; Ghosh, A.; Pal, S. *J. Appl. Polym. Sci.* **2015**, *131131*, 40039.
3. Liu, Y. H.; Zhang, F. H.; Ru, Y. Y. *Carbohydr. Polym.* **2015**, *117117*, 304.
4. Shah, S.; Sasmal, P. K.; Lee, K. B. *J. Mater. Chem. B* **2014**, *22*, 7685.
5. Song, F. F.; Li, X. Q.; Wang, Q.; Liao, L. Q.; Zhang, C. *J. Biomed. Nanotechnol.* **2014**, *1111*, 40.
6. Lee, K. Y.; Mooney, D. J. *Chem. Rev.* **2001**, *101101*, 1869.
7. Martello, F.; Tocchio, A.; Tamplenizza, M.; Gerges, I.; Pistis, V.; Recenti, R.; Bortolin, M.; Del Fabbro, M.; Argentiere, S.; Milani, P.; Lenardi, C. *Acta Biomater.* **2014**, *1010*, 1206.
8. Liu, Y.; Ibricevic, A.; Cohen, J. A.; Cohen, J. L.; Gunsten, S. P.; Freichet, J. M. J.; Walter, M. J.; Welch, M. J.; Brody, S. L. *Mol. Pharm.* **2009**, *66*, 1891.
9. Hah, H. J.; Kim, G.; Lee, Y. E. K.; Orringer, D. A.; Sagher, O.; Philbert, M. A.; Kopelman, R. *Macromol. Biosci.* **2011**, *1111*, 90.
10. Zhang, J. J.; Tokatlian, T.; Zhong, J.; Ng, Q. K. T.; Patterson, M.; Lowry, W. E. S.; Carmichael, T.; Segura, T. *Adv. Mater.* **2011**, *2323*, 5098.
11. Kopecek, J. *J. Polym. Sci. A* **2009**, *4747*, 5929.
12. McGlohorn, J. B.; Grimes, L. W.; Webster, S. S.; Burg, K. J. L. *J. Biomed. Mater. Res.* **2003**, *66A66A*, 441.
13. Tan, H. P.; Chu, C. R.; Payne, K. A.; Marra, K. G. *Biomaterials* **2009**, *3030*, 2499.
14. DeFail, A. J.; Chu, C. R.; Izzo, N.; Marra., K. G. *Biomaterials* **2006**, *2727*, 1579.
15. Josef, E.; Zilberman, M.; Bianco-Peled, H. *Acta Biomater.* **2010**, *66*, 4642.
16. Rodriguez, R.; Alvarez-Lorenzo, C.; Concheiro, A. *Euro. J. Pharm. Sci.* **2003**, *2020*, 429.
17. Liu, J. H.; Li, L.; Cai, Y. Y. *Euro. Polym. J.* **2006**, *4242*, 1767.
18. Yan, H.; Tsujii, K. *Colloids Surf. B Biointerfaces* **2005**, *4646*, 142.
19. Horn, D.; Rieger, J. *Angew. Chem. Int. Ed.* **2001**, *4040*, 4330.
20. Wang, J. X.; Zhang, Z. B.; Le, Y.; Zhao, H.; Chen, J. F. *Nanotechnology* **2011**, *2222*, 305101.
21. Lei, Y. G.; Gojgini, S.; Lam, J.; Segura, T. *Biomaterials* **2011**, *3232*, 39.
22. Singh, B.; Sharma, V. *Carbohydr. Polym.* **2014**, *101101*, 928.
23. Maswadeh, H. M.; Semreen, M. H.; Abdulhalim, A. A. *Acta Pol. Pharm.* **2006**, *6363*, 63.
24. Sullad, A. G.; Manjeshwar, L. S.; Aminabhavi, T. M. *Ind. Eng. Chem. Res.* **2010**, *4949*, 7323.